Talanta 128 (2014) 44–50

Contents lists available at ScienceDirect

Talanta

journal homepage: www.elsevier.com/locate/talanta

Detection of heavy-metal ions using liquid crystal droplet patterns modulated by interaction between negatively charged carboxylate and heavy-metal cations

Gyeo-Re Han, Chang-Hyun Jang*

Department of Chemistry, Gachon University, Seongnam-Si, Gyeonggi-Do 461-701, Korea

ARTICLE INFO

Article history:
Received 9 January 2014
Received in revised form
5 April 2014
Accepted 17 April 2014
Available online 26 April 2014

Keywords:
Liquid crystals
LC droplet pattern
Detection
Heavy-metal ion

ABSTRACT

Herein, we demonstrated a simple, sensitive, and rapid label-free detection method for heavy-metal (HM) ions using liquid crystal (LC) droplet patterns on a solid surface. Stearic-acid-doped LC droplet patterns were spontaneously generated on an *n*-octyltrichlorosilane (OTS)-treated glass substrate by evaporating a solution of the nematic LC, 4-cyano-4′-pentylbiphenyl (5CB), dissolved in heptane. The optical appearance of the droplet patterns was a dark crossed texture when in contact with air, which represents the homeotropic orientation of the LC. This was caused by the steric interaction between the LC molecules and the alkyl chains of the OTS-treated surface. The dark crossed appearance of the acid-doped LC patterns was maintained after the addition of phosphate buffered saline (PBS) solution (pH 8.1 at 25 °C). The deprotonated stearic-acid molecules self-assembled through the LC/aqueous interface, thereby supporting the homeotropic anchoring of 5CB. However, the optical image of the acid-doped LC droplet patterns incubated with PBS containing HM ions appeared bright, indicating a planar orientation of 5CB at the aqueous/LC droplet interface. This dark to bright transition of the LC patterns was caused by HM ions attached to the deprotonated carboxylate moiety, followed by the sequential interruption of the self-assembly of the stearic acid at the LC/aqueous interface. The results showed that the acid-doped LC pattern system not only enabled the highly sensitive detection of HM ions at a sub-nanomolar concentration but it also facilitated rapid detection (< 10 min) with simple procedures.

1. Introduction

In recent decades, the environmental problems caused by rapid and intensive industrialization and urbanization are receiving tremendous attention worldwide. Among these problems, heavy-metal (HM)-related environmental pollution is becoming a serious problem in many countries [1–3]. Recently, it has been revealed that smog or air pollutants such as fine dust (PM 10) and ultrafine particles (PM 2.5) containing high concentration of HM ions originating from the industrial regions of one country eventually lead to environmental problems in the adjacent countries [4,5]. An optimum level of HM ions is necessary for supporting living organisms, including humans [6]. However, excessive levels of HM ions destroy the ecosystem and eventually affect human health when these ions are accumulated in the body [6]. The toxigenic or carcinogenic effects of the HM ions accumulated in the body have been extensively reported [7,8].

In this context, many efforts have been made to monitor HM-ion concentrations by conventional analytical methods, i.e., atomic absorption/emission spectroscopy [9], inductively coupled plasma mass spectrometry [10], cold vapor atomic fluorescence spectroscopy [11], and electrochemical sensing [12]. Although these methods have contributed to the sensitive detection of HM ions, they have several limitations as well, such as the need for expensive and complex instrumentation and sophisticated and time-consuming chemical processes, which have imposed a restricted utility toward on-site HM-ion detection platforms that require portability, low cost, high sensitivity, and rapid detection [13–16].

Over the years, liquid crystals have been broadly studied as promising sensing materials that can replace conventional analytical methods for point-of-care detection [17–23]. Because of their anisotropic properties, orientation behavior, and molecular sensitivity, which enable the transduction of nanoscopic biochemical interactions into optical signals, various sensing strategies have been established for detecting parameters such as enzymatic activity [24–25], biomolecular interactions [17,18], and polymerization [19]. However, several limitations of previously explored LC-based sensing techniques, i.e., a relatively high detection limit,

* Corresponding author. Tel.: +82 31 750 8555.
E-mail address: chjang4u@gachon.ac.kr (C.-H. Jang).

http://dx.doi.org/10.1016/j.talanta.2014.04.026
0039-9140/

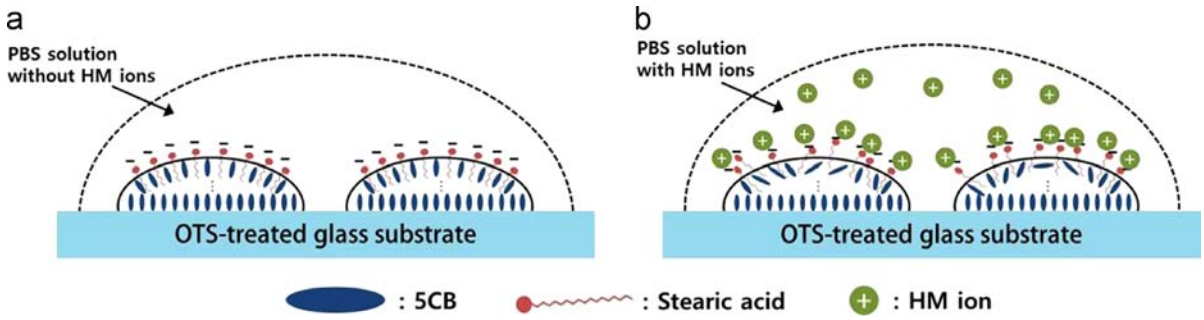

Fig. 1. Schematic illustration of orientation state of stearic-acid-doped 5CB at LC/aqueous solution interface: (a) without HM ions and (b) with HM ions.

instability of the LC/aqueous solution interface, large sample volumes, and long detection times, must be overcome. To this end, our group recently developed a new LC-based detection platform that uses surface-anchored LC droplet patterns spontaneously formed on solid surfaces [26]. Coupled with an improved stability and surface area, which should greatly improve both the sensitivity and the response time to analytes, two distinctive optical appearances, representing the orientation state of the LCs, have suggested the promising possibility of applying the LC droplet patterns as a biochemical sensing platform.

In this study, we demonstrated the sensing ability of the LC droplet patterns by investigating the orientation behavior of acid-doped LCs after the introduction of HM ions. A deprotonated stearic-acid moiety that self-assembled at the LC/aqueous solution interface was employed to induce a homeotropic anchoring of the LCs and to subsequently interact with HM ions. A dark crossed appearance, which represents the homeotropic orientation of the LCs, was observed after incubating with phosphate buffered saline (PBS) solution (pH 8.1 at 25 °C) (Fig. 1a). However, a bright, fan-shaped appearance, corresponding to a planar orientation of the LCs, was observed when the LC droplet patterns were incubated with PBS solution containing HM ions (Fig. 1b). The optical and orientation changes of the LC droplet patterns were attributed to the interaction of the HM ions with the deprotonated acid head groups and the consequent interruption of the self-assembly of the acid molecules at the LC/aqueous interface. The result of this study suggests that the LC droplet patterns can be used to build LC-based, real-time, label-free sensors that can sensitively detect HM ions with a simple method.

2. Experimental details

2.1. Materials

Glass microscope slides were obtained from Matunami (S-1215, Japan). Nematic liquid crystal 4-cyano-4′-pentylbiphenyl (5CB) was purchased from Tokyo Chemical Industry Co., Ltd. (C1555, Japan). Sulfuric acid, sodium hydroxide, hydrogen peroxide (30% v/v), and anhydrous *n*-heptane were purchased from Daejung Chemicals & Metals Co., Ltd. Octyltrichlorosilane (OTS), cobalt(II) chloride hexahydrate (60820), copper(II) chloride dihydrate (C3279), calcium chloride dehydrate (C3306), magnesium chloride hexahydrate (M2393) and phosphate buffered saline (PBS) (10^{-2} M phosphate, 1.38×10^{-3} M NaCl, 2.70×10^{-3} M KCl; pH = 7.4 at 25 °C) were obtained from Sigma-Aldrich (St. Louis, MO, USA). All aqueous solutions were prepared with high-purity deionized water (18 MΩ cm) generated using a Milli-Q water purification system (Millipore, Bedford, MA, USA). Especially, as a standard solution, 10^{-4} M solutions of each metal ions were prepared using 10^{-3} M PBS (pH 8.1 at 25 °C), and they were sequentially diluted with 10^{-3} M PBS solution (pH 8.1 at 25 °C) to make lower concentrations of the metal solutions.

2.2. Cleaning of substrates

Glass microscope slides and silicon wafers were cleaned using a piranha solution (70% H_2SO_4/30% H_2O_2) for 1 h at 80 °C. After removal from the cleaning solution, the substrates were rinsed with 500 mL of each deionized water, ethanol, and methanol, and dried under a stream of gaseous N_2. The cleaned substrates were then stored overnight in an oven at 120 °C.

2.3. Preparation of OTS-functionalized silica substrate

The piranha-cleaned glass slides and silicon wafers were immersed into an OTS/*n*-heptane solution for 30 min. The substrates were then rinsed with methylene chloride and dried under a stream of N_2. Next, the OTS-treated glass slides were tested to evaluate whether they could induce homeotropic alignment of 5CB. In order to observe optical images of 5CB in contact with the OTS-treated glass surface, 5CB optical cell was fabricated by spacing two OTS-treated glasses (facing each other) ~12 μm apart using thin strips of plastic wrap. The edges of the optical cell were held together with clips, and were heated to 40 °C. Then, 5CB, heated to its isotropic phase, was spontaneously injected into vacant space of the optical cell by capillary force. The optical cell was cooled to 25 °C for inducing the phase transition of 5CB from isotropic to nematic. If the 5CB aligned homeotropic state, the optical image appears dark. Any slide that did not display the dark image (homeotropic alignment of 5CB) was discarded.

2.4. Preparation of stearic-acid-doped LC droplet patterns on solid surface

After mixing a solution of 1% (v/v) 5CB in heptane with 0.005% stearic acid dissolved in heptane, 3 μL of the mixed solution was dispensed onto an OTS-treated glass slide. After evaporation of the organic solvent, a drop of HM-containing aqueous solution (4 μL) was introduced onto the LC droplet patterns at 25 °C. During the incubation, a humidity of the enclosed reaction environment was controlled using wetted tissue to prevent the concentration change in HM solution, which could be triggered by the evaporation of solvent.

2.5. Imaging of LC textures

A polarized light microscope (ECLIPSE LV100POL, Nikon, Tokyo, Japan) was used to image the optical textures formed by light transmitted through the optical cells filled with nematic 5CB. All the images were obtained using a 10× objective lens under crossed polarizers. The images of the optical appearance of each liquid crystal cell were captured using a digital camera (DS-2Mv,

Nikon, Tokyo, Japan) attached to the polarized light microscope at a resolution of 1600 × 1200 pixels, a gain of 1.40 ×, and a shutter speed of 1/10 s.

3. Results and discussion

3.1. Orientation behavior of acid-doped 5CB droplet pattern at LC/aqueous solution interface

Here, we used stearic acid, a saturated fatty acid molecule that contains both a long hydrophobic chain and a hydrophilic head group, to regulate the orientation state of 5CB at the LC droplet pattern/aqueous solution interface. Previously, the effect of a pH-responsive amphiphilic carboxylate molecule on the anchoring state of 5CB was extensively investigated at the LC/aqueous solution interface [27,28]. An increase in pH promoted the deprotonation of the carboxylate head groups and changed the optical appearance of the 5CB domains (from bright to dark) by the orientation transition of 5CB (from planar to homeotropic) at the LC/aqueous solution interface. On the basis of this result, we hypothesized that doping 5CB with stearic acid would anchor the orientation of the 5CB molecules in the homeotropic state after the introduction of an aqueous solution at the 5CB droplet pattern/aqueous solution interface.

To prove this hypothesis, we compared the optical response of the acid-doped 5CB droplet patterns with that of the pure 5CB droplet patterns after incubating the patterns with 10^{-3} M PBS solution. To increase the proportion of deprotonated stearic acid at the interface, the pH of the PBS solution was adjusted to 8.1. Moreover, only 5CB droplet patterns with size 60–80 μm were used. Fig. 2a and b shows the orientation response of the pure 5CB droplet patterns on the OTS surface before and after incubating with 10^{-3} M PBS solution (pH 8.1). The pure 5CB droplet pattern itself presented a dark crossed optical texture, which suggested the homeotropic anchoring of 5CB at the LC/air interface (Fig. 2a). In this case, the homeotropic orientation of 5CB at the LC droplet pattern/air interface arose from the homeotropic anchoring of the 5CB molecules inserted between the octyl chains of the OTS. However, after incubating the 5CB droplet patterns with the PBS solution (pH 8.1, 25 °C), the optical appearance of the 5CB droplet pattern changed from dark crossed to a bright fan-shaped texture, which represented a planar orientation of 5CB at the LC/aqueous interface. In contrast, in the case of stearic-acid doped 5CB, we observed that the dark crossed optical texture of the 5CB droplet patterns was maintained even after the introduction of a drop of PBS solution on the 5CB droplet pattern (Fig. 2c and d). Compared to Fig. 2c, a slight increase in brightness and resolution of the dark-crossed pattern was recognized in Fig. 2d. Considering the constant image capture condition on both images, it is estimated that the enhancement was caused by a consolidation of the homeotropic anchoring of 5CB at the 5CB droplet pattern/aqueous solution interface. Although the optical texture of the droplet pattern showed a fan-shaped texture immediately after coming in contact with the PBS solutions to acid-doped 5CB droplet patterns, the subsequent deprotonation of the carboxyl group into carboxylate (negatively charged) ultimately induced the homeotropic anchoring of 5CB at the 5CB droplet pattern/aqueous solution interface in 5 min. The dark crossed shape was then maintained until the PBS solution evaporated (> 1 h). From these results, we concluded that the homeotropic anchoring of the stearic-acid-doped 5CB at the LC/aqueous solution interface was mediated by the steric interaction between the alkyl chains of the self-assembled stearic acid and the 5CB molecules.

3.2. Orientation transition of acid-doped 5CB mediated by interaction between negatively charged carboxylate and HM cations

Hu et al. investigated the orientation change of 5CB induced by the electrostatic interactions between a negatively charged phospholipid and positively charged poly-L-lysine (PLL) [29]. They induced the orientation transition of 5CB (from homeotropic to planar) at the LC/aqueous solution interface by introducing positively charged PLL to the LC/aqueous solution interface already decorated with negatively charged phospholipid. As a result, they succeeded in constructing a trypsin-detection system based on the electrostatic interactions and their effect on the orientation state of 5CB. On the other hand, Hyun et al., by using Fourier transform

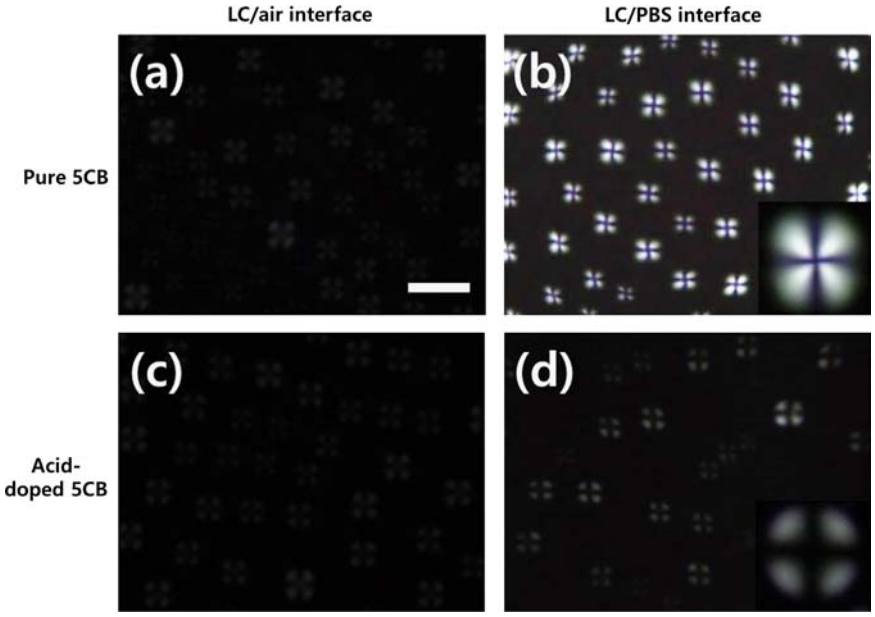

Fig. 2. Optical images of pure 5CB (a and b) and acid-doped 5CB (c and d) observed under polarized light: (a) pure 5CB without 10^{-3} M PBS solution (pH 8.1 at 25 °C); (b) pure 5CB with 10^{-3} M PBS solution; (c) acid-doped 5CB without 10^{-3} M PBS solution; and (d) acid-doped 5CB with 10^{-3} M PBS solution. Subset images inserted in (b) and (d), respectively, represent bright fan-shaped texture and dark crossed texture of a single 5CB droplet pattern. Size of scale bar is 200 μm.

infrared spectroscopy and a modeling method which exploited electrochemistry and thermodynamics, suggested that each metal ion shows different selectivity to the surface of stearic acidic monolayer [30]. The result of the study revealed that surface ion adsorption constant of HM ions are usually relatively higher than that of other metal ions. Based on the results of the studies, we proposed that charge interaction-dependent detection system can be used to detect HM cations using stearic-acid-doped 5CB droplet patterns. Although the molecular size of the HM ion was extremely small compared to the PLL molecule, we expected that the detection of HM ions would be possible considering the large surface area available to react with analytes. Therefore, we hypothesized that the introduction of HM ions to the acid-doped 5CB droplet patterns would disturb the self-assembly of the deprotonated acid molecules by the electrostatic interaction between the positively charged HM ions and the negatively charged carboxylate head groups. However, for the reason that the detection mechanism mainly depends on the electrostatic interaction, selectivity of the detection system to HM ions was tested against to alkaline earth metals (Ca^{2+} and Mg^{2+}). To test this hypothesis, 10^{-4} M solution of cobalt(II) chloride, copper(II) chloride, calcium chloride and magnesium chloride in 10^{-3} M PBS (pH 8.1 at 25 °C) were prepared as a stock solution. After dispensing 3 μL of the stearic-acid-doped 5CB in heptane onto the OTS-treated glass substrate, 4 μL of the stock solutions were incubated on the 5CB droplet patterns, which had a size distribution in the range 60–80 μm. At the concentration, no optical difference was observed between HM ions and the other ions (Fig. S1). The reason was due to the excessive absorption of the metal ions to the carboxylate molecules embedded in the interface of the 5CB droplet pattern/PBS solution.

For further investigation on the selective response of the 5CB droplet patterns to HM ions, we monitored the state of pattern transition by lowering the concentration of the metal solutions. Fig. 3a–c shows concentration dependent optical appearance of the 5CB droplet patterns when the surfaces were respectively incubated with 5.048×10^{-7} M (Fig. 3a), 5.039×10^{-7} M (Fig. 3b) and 5.029×10^{-7} M (Fig. 3c) of calcium chloride dissolved in 10^{-3} M PBS solutions. Compared to the distinctive bright fan-shaped (Fig. 3a) and dark crossed (Fig. 3c) texture of the pattern, the intermediate state which contains both distorted bright fan-shaped texture and dark crossed one was simultaneously observed on Fig. 3b. On the experiment which employed the calcium chloride solution lower than 5.029×10^{-7} M, the dark crossed texture was uniformly maintained (images are not shown). Based on the result, the calcium ion concentration which shows no reaction capacity with the 5CB pattern was confirmed in the vicinity of 5.039×10^{-7} M. Meanwhile, Fig. 3d–f, correspondingly, shows the representative optical textures of the 5CB droplet patterns after incubating the patterns with 1.015×10^{-7} M, 1.008×10^{-7} M and 10^{-7} M of magnesium chloride in 10^{-3} M PBS. The surface of the patterns contacted with 1.015×10^{-7} M and 10^{-7} M revealed distinctive responses of bright fan-shaped texture (Fig. 3d; 1.015×10^{-7} M) and dark crossed texture (Fig. 3f; 100.0×10^{-9} M). However, the patterns, incubated with the 10^{-7} M of magnesium chloride solution, revealed coexistence of distinctive dark crossed texture and intermediate state of pattern (Fig. 3e). After incubating the surface with the magnesium chloride solutions lower than 1.008×10^{-7} M, the dark crossed appearance was consistently observed (images are not shown). The result implies that the transition of the pattern was occurred in the vicinity of 1.015×10^{-7} M magnesium ion concentration. It is estimated that the difference between the threshold concentration of calcium ion (5.039×10^{-7} M) and magnesium ion (1.008×10^{-7} M) is originated from the simultaneous effect of (i) a difference in electronegativity, χ, of the atoms (χ of calcium: 1.00; χ of magnesium: 1.31 in Pauling scale) and (ii) a difference in ionic radius which affects to Coulomb force. In conclusion, a concentration of 10^{-7} M was determined as criteria which could give a HM selectivity of the detection system.

In order to investigate the selectivity to HM ions at the concentration lower than 10^{-7} M, we incubated the 5CB droplet patterns with cobalt(II) chloride and copper (II) chloride, respectively. Fig. 4a and b shows the optical appearance of the 5CB droplet patterns before (Fig. 4a) and after (Fig. 4b) incubating the surface with 10^{-7} M cobalt(II) chloride solution. After introducing the solution containing cobalt ions to the 5CB patterns, we immediately observed an optical transition in the appearance of

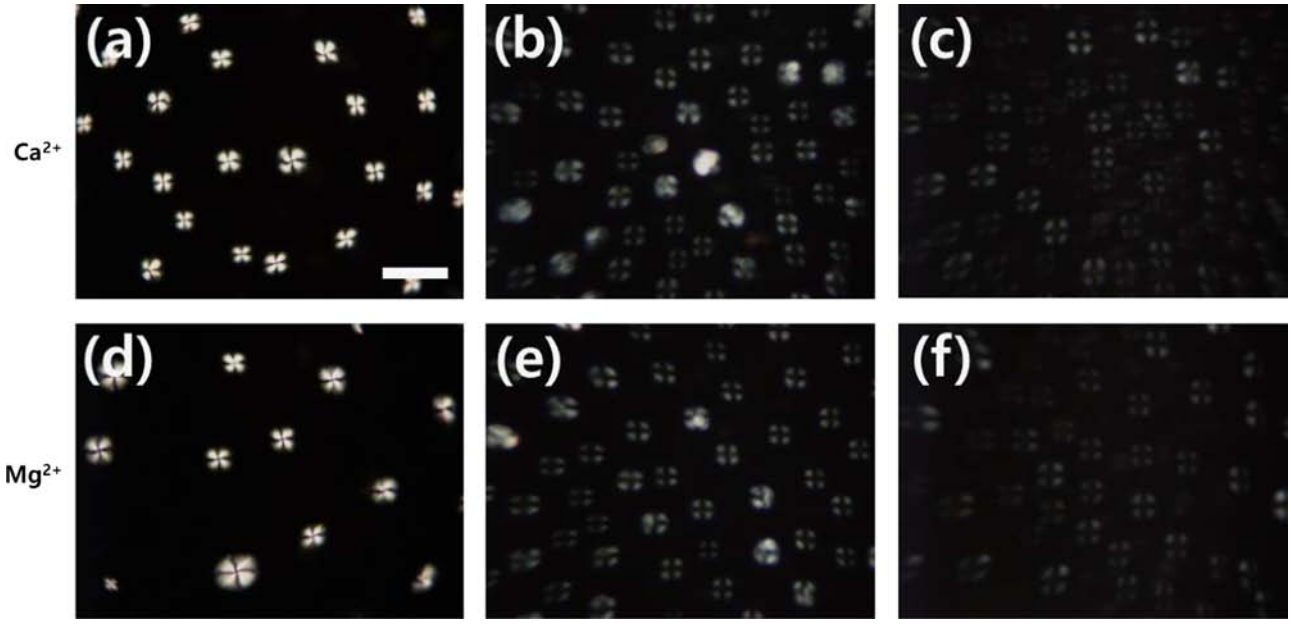

Fig. 3. Polarized light microscopy images of acid-doped 5CB droplet patterns incubated with: calcium chloride in 10^{-3} M PBS solution (pH 8.1 at 25 °C) at a concentration of (a) 5.048×10^{-7} M, (b) 5.039×10^{-7} M, and (c) 5.029×10^{-7} M; magnesium chloride in 10^{-3} M PBS solution (pH 8.1 at 25 °C) at a concentration of (d) 1.015×10^{-7} M, (e) 1.008×10^{-7} M, and (f) 10^{-7} M. Size of scale bar is 200 μm.

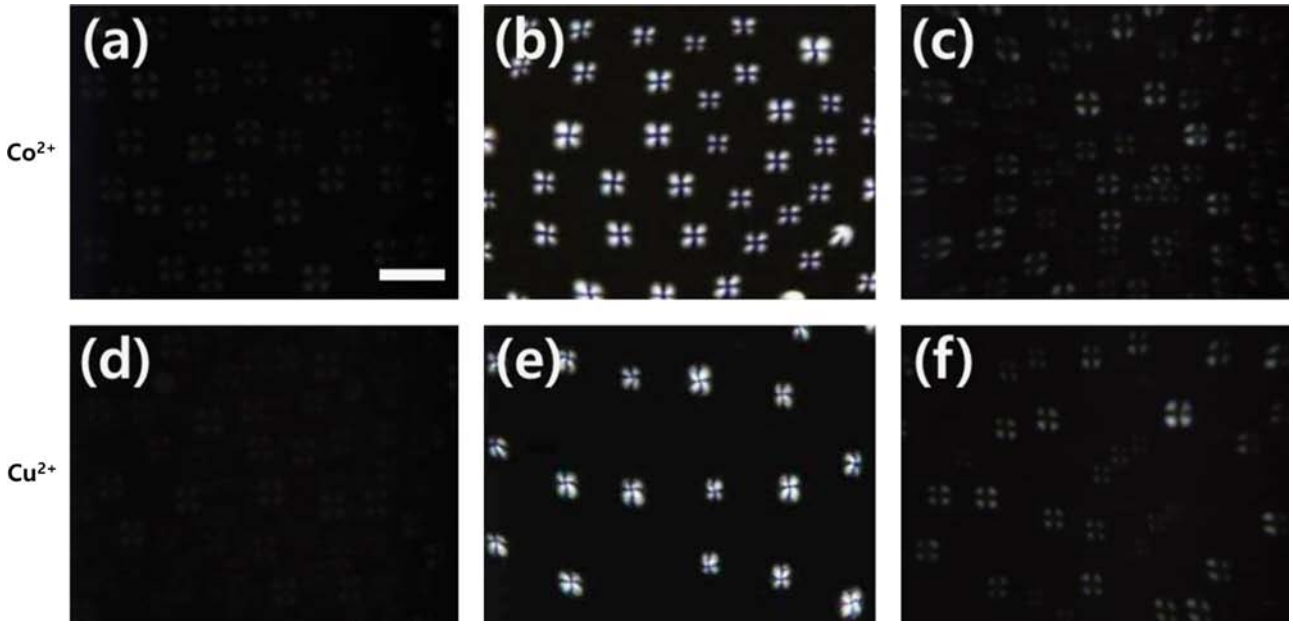

Fig. 4. Polarized light microscopy images of acid-doped 5CB droplet patterns (a and d) after incubating the surface with: (b) 10^{-7} M cobalt(II) chloride in 10^{-3} M PBS solution (pH 8.1 at 25 °C) and (c) 10^{-3} M PBS solution (pH 8.1 at 25 °C); (e) 10^{-7} M copper(II) chloride in 10^{-3} M PBS solution (pH 8.1 at 25 °C) and (f) 10^{-3} M PBS solution (pH 8.1 at 25 °C). Size of scale bar is 200 μm.

the 5CB droplet patterns (< 30 s): from a dark crossed pattern (Fig. 4a) to a bright fan-shaped texture (Fig. 4b), corresponding to a planar orientation of 5CB at the LC/aqueous solution interface. The bright texture was maintained until the entire aqueous droplet evaporated. However, in a control experiment incubating the acid-doped 5CB droplet patterns with 10^{-3} M PBS (pH 8.1 at 25 °C), no optical transition was detected (Fig. 4c). Similarly, the dark crossed optical appearance of the 5CB pattern (Fig. 4d) immediately changed to a bright appearance (Fig. 4e) after contacting the 5CB patterns with 10^{-7} M copper(II) chloride solution. In contrast, there was no transition in the optical response of the control experiment (Fig. 4f).

Contrary to the dark crossed texture caused by 10^{-7} M calcium chloride and magnesium chloride in PBS solution, the HM solutions of 10^{-7} M triggered the optical transition (from dark crossed to bright fan-shaped) of the 5CB droplet pattern. The results suggest that the optical transition originated from the electrostatic interactions between the negatively charged carboxylate head groups of the stearic acid and the positively charged HM cations. We attributed the orientation transition (from homeotropic to planar) of 5CB at the LC/aqueous solution interface to the interruption of the steric interaction between 5CB and the deprotonated stearic-acid molecules, induced by the coupling of the carboxylate head group with the HM ions. The selective response of the pattern toward HM ions corresponds to their higher affinity toward the stearic acid molecule compared to other metal ions [30]. Consequently, we demonstrated that it is possible to detect HM ions using stearic-acid-doped 5CB droplet patterns with selectivity.

3.3. Detection limits of HM ions

In order to find detection limits of the HM ions, we continued our investigation on the orientation behavior of the acid-doped 5CB droplet patterns using lowered concentrations of HM ions. In a previous study, divalent copper ions were detected using an LC biosensor based on the enzymatic activity of urease [28]. However, the reported detection limit of 10^{-5} M and reaction time of 1 h need improvement before the sensing platform can be considered useful for both on-site and real-time HM monitoring applications. Thus, we first set a reaction time of 10 min for providing sufficient time for the interaction between the HM ions and the deprotonated stearic acid to occur at the interface, and then we measured the detection limit of our system for the HM ions. All the images were captured after incubating the HM solutions for 10 min.

Fig. 5a–f, correspondingly, shows the optical images of the 5CB droplet patterns after incubating the surface with 10^{-8} M, 10^{-9} M, 10^{-10} M, 7.00×10^{-11} M, 5.00×10^{-11} M and 3.00×10^{-11} M cobalt (II) chloride in 10^{-3} M PBS solution (pH 8.1 at 25 °C). As shown in Fig. 5a–c, we observed the bright fan-shaped texture when the concentration of the cobalt(II) chloride solution was lowered to 10^{-10} M. However, when 10^{-11} M cobalt(II) chloride solution was introduced to the sensor surface, dark crossed texture which corresponds to the homeotropic anchoring of 5CB at the LC/aqueous solution interface was observed. We subdivided the concentration of the cobalt(II) chloride solution between 10^{-10} M and 10^{-11} M, and then gradually closed a range of the detection limit. Compared to the bright fan-shaped texture and entirely dark crossed texture shown in Fig. 5d (7.00×10^{-11} M) and f (3.00×10^{-11} M), a mixture of dark crossed and distorted bright fan-shaped texture was observed (Fig. 5e). On Fig. 5e, the distorted fan-shaped pattern is shown as a bright circular spot because the focus of the microscope was optimized to dark crossed texture. The results suggest that 5.00×10^{-11} M cobalt(II) chloride solution was not sufficient to entirely change the orientation of 5CB (from homeotropic to planar). Based on the result, the detection limit of this system to cobalt cation was estimated to in the range of 5.00×10^{-11}–7.00×10^{-11} M.

To provide a general applicability of this system toward HM-ion detection, the detection limit of the 5CB droplet pattern system toward copper cations was investigated. Fig. 6a–f, in sequence, represent the optical responses of the 5CB droplet pattern which correspond to 10^{-8} M, 10^{-9} M, 10^{-10} M, 5.00×10^{-11} M, 3.00×10^{-11} and 10^{-11} M of copper(II) chloride in 10^{-3} M PBS solution. As shown in Fig. 6a–d, the bright fan-shaped optical textures (including distorted bright fan-shaped) which correspond to the planar orientation of 5CB at LC/aqueous solution interface was consistently observed until the concentration of the copper(II) chloride solution was lowered to 5.00×10^{-11} M. When the patters

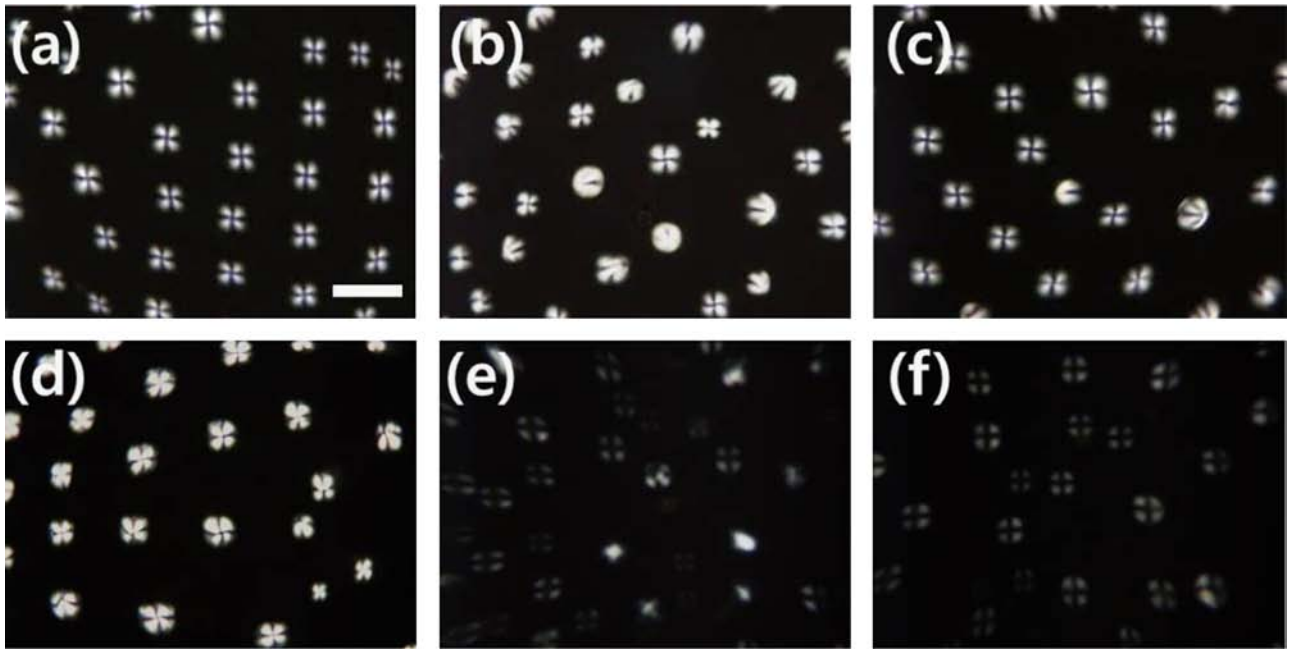

Fig. 5. Polarized light microscopy images of acid-doped 5CB droplet patterns incubated with cobalt(II) chloride in 10^{-3} M PBS solution (pH 8.1 at 25 °C) at a concentration of (a) 10^{-8} M, (b) 10^{-9} M, (c) 10^{-10} M, (d) 7.00×10^{-11} M, (e) 5.00×10^{-11} M and (f) 3.00×10^{-11} M. Size of scale bar is 200 μm.

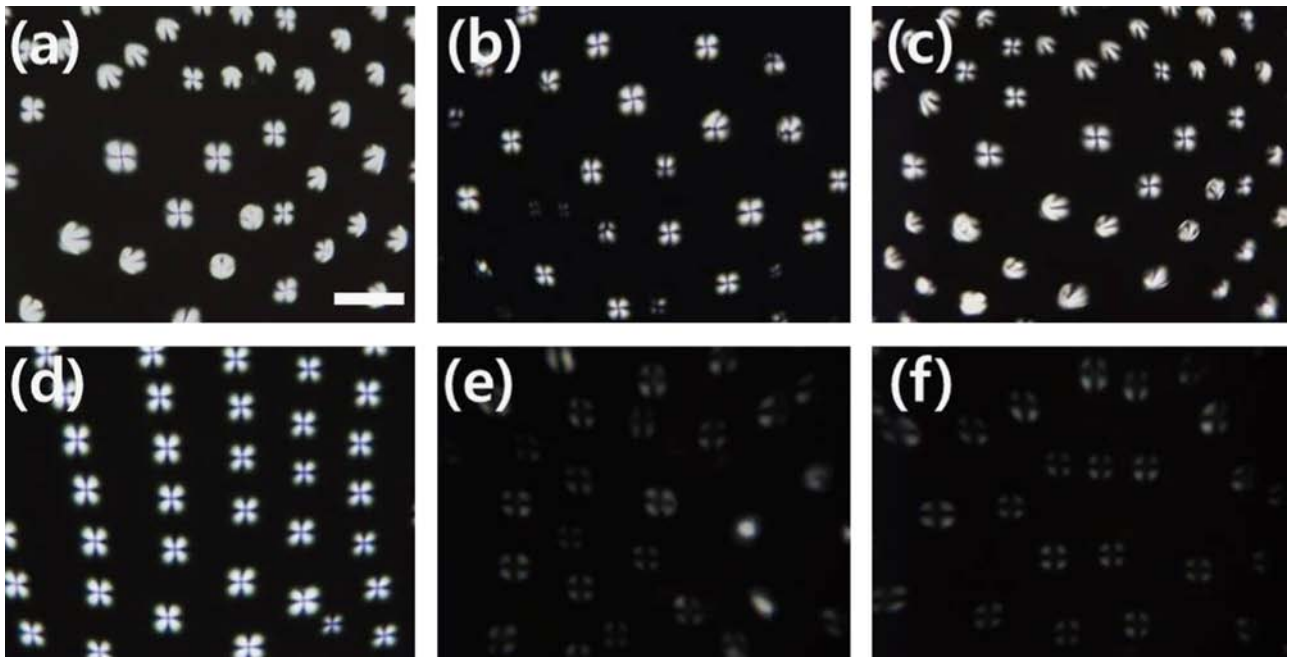

Fig. 6. Polarized light microscopy images of acid-doped 5CB droplet patterns incubated with copper(II) chloride in 10^{-3} M PBS solution (pH 8.1 at 25 °C) with a concentration of (a) 10^{-8} M, (b) 10^{-9} M, (c) 10^{-10} M, (d) 5.00×10^{-11} M, (e) 3.00×10^{-11} M and (f) 10^{-11} M. Size of scale bar is 200 μm.

were incubated with 3.00×10^{-11} M copper(II) chloride solution, the intermediate state (combination of the dark crossed and distorted bright fan-shaped texture of patterns) was observed (Fig. 6e). However, entirely dark crossed textures which represent the homeotropic anchoring of 5CB was observed after incubating the sensor surface with 10^{-11} M copper(II) chloride solution (Fig. 6f). Considering the weakened response capacity of the patterns as the function of copper cation concentrations, the detection limit of the system toward the copper ion was revealed in the range of 3.00×10^{-11}–5.00×10^{-11} M. Here, a minute difference in the range of detection limit, between cobalt and copper cation, was revealed. Considering the same level of ionic strength at the same concentration of HM ions but in different type, it is estimated that the disparity in detection limit is originated from the different adsorption affinity of each HM ions toward the stearic acid molecules, which is affected by: (i) a narrow difference in electronegativity of cobalt (1.88) and copper (1.90); (ii) a subtle difference in Coulomb force between the heavy metal ions and deprotonated carboxylic groups.

4. Conclusion

In summary, we have developed a convenient, real-time analytical method for the label-free detection of HM ions using

the optical response of stearic-acid-doped 5CB droplet patterns. In the presence of HM ions, the acid-doped 5CB droplet patterns appeared bright with a fan-shaped texture, which corresponds to the planar orientation of 5CB at the LC/aqueous solution interface. However, the dark crossed optical texture of the 5CB droplet pattern was maintained in the absence of HM ions, as well as in the presence of alkaline earth metals. The ranges of the detection limit were respectively determined to 5.00×10^{-11}–7.00×10^{-11} M (for cobalt cation) and 3.00×10^{-11}–5.00×10^{-11} M (for copper cation). In conclusion, these results demonstrate that the acid-doped 5CB droplet pattern could be used to detect HM ions.

Acknowledgments

This study was supported by the Gachon University Research Fund 2014 (GCU-2014-R043).

Appendix A. Supplementary material

Supplementary data associated with this article can be found in the online version at http://dx.doi.org/10.1016/j.talanta.2014.04.026.

References

[1] Y. Hu, X. Liu, K. Shin, E.Y. Zeng, H. Cheng, Environ. Sci. Pollut. Res. 20 (2012) 6150–6159.
[2] F. Mireles, J.I. Davila, J.L. Pinedo, E. Reyes, R.J. Speakman, M.D. Glascock, Microchem. J. 103 (2012) 158–164.
[3] B. Wei, L. Yang, Microchem. J. 94 (2010) 99–107.
[4] Q. Qang, X.H. Bi, J.H. Wu, Y.F. Zhang, Y.C. Feng, Environ. Monit. Assess. 185 (2013) 1473–1482.
[5] J.S. Pastuszka, W. Rogula-Kozłowska, E. Zajusz-Zubek, Environ. Monit. Assess. 168 (2010) 613–627.
[6] G. Aragay, J. Pons, A. Merkoçi, Chem. Rev. 111 (2011) 3433–3458.
[7] J.W. Hamilton, R.C. Kaltreider, O.V. Bajenova, M.A. Ihnat, J. McCaffrey, B.W. Turpie, E.E. Rowell, J. Oh, M.J. Nemeth, C.A. Pesce, J.P. Lariviere, J. Environ. Health 106 (1998) 1005–1015.
[8] B.L. Vallee, D.D. Ulmer, Annu. Rev. Biochem. 41 (1972) 92–128.
[9] A. Orhan, Talanta 65 (2005) 672–677.
[10] S. Ashoka, B.M. Peake, G. Bremner, K.J. Hageman, M.R. Reid, Anal. Chim. Acta 653 (2009) 191–199.
[11] P.R. Aranda, P.H. Pacheco, R.A. Olsina, L.D. Martinez, R.A. Gil, J. Anal. At. Spectrom. 24 (2009) 1441–1445.
[12] D. Potesil, J. Petrlova, V. Adam, J. Vacek, B. Klejdus, J. Zehnalek, L. Trnkova, L. Havel, R. Kizek, J. Chromatogr. A 1084 (2005) 134–144.
[13] R.B. Thompson, B.P. Maliwal, V.L. Feliccia, C.A. Fierke, K. McCall, Anal. Chem. 80 (1998) 4717–4723.
[14] I. Bontidean, C. Berggren, G. Johansson, E. Csoregi, B. Mattiasson, J.R. Lloyd, K.J. Jakeman, N.L. Brown, Anal. Chem. 80 (1998) 4162–4169.
[15] S. Han, M. Zhu, Z. Yuan, X. Li, Biosens. Bioelectron. 16 (2001) 9–16.
[16] G.L. Turdean, Int. J. Electrochem. 2011 (2011) 343125.
[17] G.R. Han, C.H. Jang, Colloids Surf. B Biointerfaces 116 (2014) 147–152.
[18] G.R. Han, C.H. Jang, Colloids Surf. B Biointerfaces 94 (2012) 89–94.
[19] G.R. Han, C.H. Jang, Colloid Polym. Sci. 291 (2013) 2689–2696.
[20] Q.Z. Hu, C.H. Jang, Talanta 99 (2012) 36–39.
[21] Q.Z. Hu, C.H. Jang, Analyst 137 (2012) 5204–5207.
[22] Y. Bai, N.L. Abbott, Langmuir 27 (2011) 5719–5738.
[23] A. Hussain, A.S. Pina, A.C.A. Roque, Biosens. Bioelectron. 25 (2009) 1–8.
[24] D. Liu, Q.Z. Hu, C.H. Jang, Colloids Surf. B Biointerfaces 108 (2013) 142–146.
[25] S. Liao, Y. Qiao, W. Han, Z. Xie, Z. Wu, G. Shen, R. Yu, Anal. Chem. 84 (2012) 45–49.
[26] Q.Z. Hu, C.H. Jang, Soft Matter 9 (2013) 5779–5784.
[27] D. Liu, C.H. Jang, Sens. Actuators B 193 (2014) 770–773.
[28] Q.Z. Hu, C.H. Jang, Colloids Surf. B Biointerfaces 88 (2011) 622–626.
[29] Q.Z. Hu, C.H. Jang, ACS Appl. Mater. Interfaces 4 (2012) 1791–1795.
[30] J.Y. Hyun, G.S. Lee, T.Y. Kim, D.J. Ahn, Korean J. Chem. Eng. 14 (1997) 533–540.